International Journal of Electric Power and Energy Studies
ISSN: 3006-2004 (Print), ISSN: 3006-0826 (Online) | Volume 5, Number 1, Year 2026
DOI: https://doi.org/10.62051/ijepes.v5n1.03
Journal homepage: https://wepub.org/index.php/IJEPES/index

SOC Estimation Method, Application and Prospect of LFP Battery: A Review

Xiaonan Liu*

College of New Materials and New Energies, Shenzhen Technology University, Shenzhen, 518118, China
*202200302103@stumail.sztu.edu.cn

ABSTRACT

The precise determination of the State of Charge is crucial for Lithium Iron Phosphate batteries, yet it continues to present significant challenges. These difficulties primarily stem from the batteries' notably flat voltage profile, considerable hysteresis effects, and their high sensitivity to thermal fluctuations and aging processes. This review systematically analyzes two dominant SOC estimation methodologies: purely data-driven models and physical-data-driven hybrid models. Data-driven approaches (e.g., DNN, LSTM) excel at capturing complex nonlinearities but lack interpretability and require substantial data. Hybrid models, combining equivalent circuit models with state estimators like Kalman filters, offer a balance of physical insight and computational efficiency, yet their accuracy often depends on offline calibration. The analysis concludes that future advancements hinge on developing online adaptive algorithms and deeply integrated hybrid strategies to enhance robustness and generalization across diverse real-world operating conditions.

KEYWORDS

Lithium Iron Phosphate Batteries; State of Charge; Battery Management System.

1. INTRODUCTION

Against the global push toward net-zero CO_2 emissions by 2050, the advancement of renewable energy technologies has taken center stage in efforts to phase out fossil fuels. The transportation sector, consistently the second-largest emitter of CO_2 over the past thirty years-only behind electricity and heat generation-plays a crucial role in this shift. With global fossil fuel reserves declining, the transition from conventional internal combustion engines to electric vehicles (EVs) appears not just inevitable but already well underway. According to the International Energy Agency (IEA), the expansion of EVs aligns strongly with the 2050 net-zero emissions trajectory. More recent IEA projections from 2024 suggest that the growth of renewable energy across transport, industry, and buildings is set to double by 2030 compared with the 2017–2023 period. Within the transport sector, renewable electricity is expected to drive half of this growth, largely spurred by the accelerating adoption of electric vehicles worldwide.

As the primary energy source for electric vehicles, rechargeable batteries must strike a delicate balance between driving range and safety-a central and ongoing challenge for the industry. Among available technologies, lithium-ion batteries (LIBs) have gradually established themselves as the leading solution, outperforming traditional options like lead-acacid and nickel-metal hydride cells with their superior energy density, high Coulombic efficiency, and minimal self-discharge. Common LIB chemistries used in today's electric vehicles include lithium cobalt oxide (LCO), lithium nickel oxide (LNO), lithium iron phosphate (LFP), lithium manganese oxide (LMO), lithium nickel cobalt

aluminum oxide (NCA), and lithium nickel manganese cobalt oxide (NMC). A comparative overview of their performance is provided in Table 1[1].

From current data, LFP batteries distinguish themselves from other lithium-ion types owing to a combination of favorable properties: enhanced safety, strong thermal stability, and relatively low cost. These advantages have made them the technology of choice for a growing number of new energy vehicle manufacturers. As of 2021, LFP cathode materials already accounted for 42% of the market, and that share is expected to climb to 51% by 2030[2].

Table 1. Typical performance parameters of commercial lithium-ion batteries.

Battery type	Voltage(V)	Specific energy(Wh/kg)	Charge(c)	Discharge(c)	Life span(hrs)
LCO	3.7-3.8	160-200	0.7-1	1	600-1000
LNO	3.6-3.8	160-200	0.7-1	1	>300
LFP	3.2-3.4	90-120	1	1	1000-2100
LMO	3.7-3.9	100-145	0.7-1	1	300-750
NCA	3.6-3.7	200-250	0.7	1	~500
NMC	3.8-4.1	150-210	0.7-1	1	1000-2100

To fully harness the potential of battery energy storage, extend service life, and reduce operational costs, electric vehicles are universally equipped with a Battery Management System (BMS). Key functions of the BMS include managing charge and discharge cycles, regulating temperature, ensuring safe operation, and accurately estimating the SOC. Among these, SOC serves as a crucial indicator: it not only informs energy management strategies within the BMS but also enables reliable predictions of remaining driving range-a feature greatly valued by users.SOC is usually defined as the percentage of remaining available electricity relative to the current maximum available capacity:

$$SOC=\frac{Q_{remaining}}{Q_{max}}\times 100\% \tag{1}$$

Currently, common SOC estimation techniques include direct measurement, model-based algorithms, and data-driven approaches. Yet, achieving reliable accuracy remains difficult due to complicating factors such as battery aging, temperature dependence, and inherent nonlinear behavior[3]. This challenge is particularly pronounced in LFP batteries, which exhibit an extremely flat voltage plateau and notable hysteresis effects -far more so than in widely used NCA and NMC batteries[4]. These characteristics complicate voltage-based estimation and create an urgent need for tailored compensation models or novel methodologies.

Given these constraints, this paper focuses specifically on LFP batteries, offering a systematic classification and critical analysis of existing SOC estimation methods. We aim to identify strengths and limitations in current approaches, thereby supporting future developments in this evolving field.

2. CHALLENGES

For NMC batteries, the charge-discharge OCV-SOC curve approximates a straight line, making the open-circuit voltage lookup table method both effective and reliable. In contrast, for LFP batteries, the deintercalation reaction of Li+ occurs through the movement of the two-phase interface between

$LiFePO_4$ (lithium-rich phase) and $FePO_4$ (lithium-deficient phase). This results in a flat voltage plateau during charge and discharge processes[5]. Minor noise signals can mask the subtle changes in OCV values, thereby rendering the commonly used open-circuit voltage lookup table method ineffective. Additionally, the errors of other estimation methods may also increase to varying degrees. Fig. 1 shows the OCV-SOC curves during charge and discharge for NMC and LFP batteries[6].

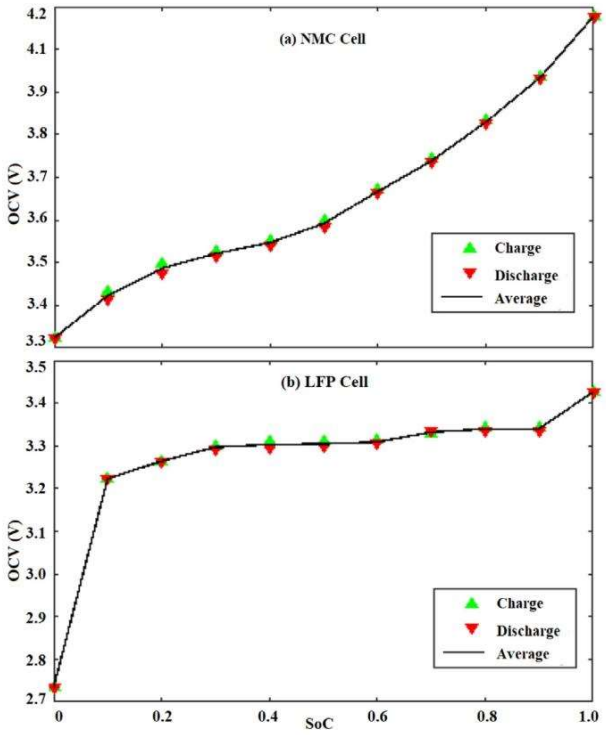

Fig. 1. OCV-SOC curve of (a) NMC and (b) LFP battery cell during charging and discharging.

Furthermore, there are multiple sources of error in SOC estimation for LFP batteries, such as hysteresis effects, temperature sensitivity, and aging impacts. The hysteresis effect refers to the voltage difference between the charge and discharge OCV-SOC curves, which do not overlap. In practice, the open-circuit voltage variation in the flat voltage region of LFP batteries is only about 0.1 V, while the voltage difference caused by hysteresis can exceed 32 mV-almost one-third of the total voltage change. As a result, the mapping relationship between OCV and SOC is closely tied to the charge-discharge history, significantly increasing SOC estimation errors[7]. To mitigate the impact of hysteresis, enhanced hysteresis models can be established and combined with methods such as Kalman filtering or neural networks to improve estimation accuracy.

Secondly, LFP batteries are highly sensitive to temperature. At low temperatures, their internal resistance and polarization voltage increase significantly, accompanied by an intensified hysteresis effect[8]. This exacerbates cumulative errors in Coulomb counting and causes abrupt estimation errors in observers like the Extended Kalman Filter (EKF). At high temperatures, battery aging accelerates, leading to capacity fade, increased internal resistance, and an overall downward shift in the plateau voltage[9], which also complicates SOC estimation.

In light of these challenges, this paper aims to provide a practical perspective on the strengths, limitations, and application prospects of physical-data-driven hybrid models and purely data-driven models for SOC estimation in LFP batteries. The remainder of this paper is structured as follows: Section 3 discusses purely data-driven models, Section 4 examines physical-data-driven hybrid models, and Section 5 provides a concluding summary.

3. PURELY DATA-DRIVEN MODELS

Purely data-driven models represent a category of modeling methods for battery SOC estimation that do not rely on the internal electrochemical mechanisms, structural parameters, or physical details of the battery. The core idea is to leverage only externally measurable variables-such as current, voltage, and temperature-and employ statistical or machine learning algorithms to establish an end-to-end mapping from these inputs to the SOC. Unlike mechanism-based or hybrid approaches, purely data-driven models do not incorporate explicit physical representations of internal battery processes. Instead, they directly extract patterns and relationships from historical operational data, focusing primarily on predicting "what is the state" or "what will happen." A diverse array of machine learning and deep learning approaches are typically employed to execute these methods. This encompasses both shallow models, like support vector machines and Gaussian process regression, and deep - structured models, including Convolutional Neural Networks, Recurrent Neural Networks, and Long Short-Term Memory networks.

In the realm of State of Charge (SOC) assessment for Lithium Iron Phosphate (LFP) batteries, solely data - based models have garnered significant interest in the past few years. This is because of their strong ability to fit non-linear relationships, the fact that they bypass intricate physical parameter determination, and their comparative resilience against the impacts of voltage plateaus. They demonstrate particular promise in applications where ample data are available, computational resources are sufficient, and real-time requirements are moderate-such as in cloud-based BMS, energy storage systems, and battery health management platforms.

However, purely data-driven models also come with inherent limitations, including low interpretability, strong dependency on the quality and representativeness of training data, limited generalization under unseen conditions, and challenges in embedded real-time deployment. Therefore, in practical applications, they are often integrated with physics-based or hybrid modeling strategies to achieve a more balanced performance in terms of accuracy, robustness, and explainability.

3.1. Traditional Data-driven Methods

Traditional data-driven methods primarily refer to machine learning models with relatively simple structures, fewer parameters, and typically no deep networks or complex automatic feature extraction mechanisms. Most of these methods originated from the early stages of machine learning development, relying on manual feature engineering and prior knowledge. They were once widely applied in scenarios with small-scale datasets, limited computational resources, or high demands for model interpretability.

In SOC estimation tasks, such methods typically use physical quantities such as current, voltage, and temperature as inputs to predict SOC values through regression or classification. Although these models can achieve satisfactory estimation results under specific conditions, they generally suffer from weaknesses in modeling temporal dynamic features, limited generalization performance, and difficulties in capturing high-dimensional nonlinear relationships. Particularly when dealing with the voltage plateau characteristics of LFP batteries and complex usage conditions, their accuracy and robustness often fall short of practical application requirements.

3.2. Deep Learning Methods

With the rapid development of artificial intelligence technology, deep learning methods have gradually emerged as one of the mainstream data-driven approaches in the field of battery SOC estimation, leveraging their exceptional non-linear fitting capabilities, automatic feature extraction mechanisms, and advantages in modeling complex temporal relationships.

These methods typically take raw or preprocessed sensor data (such as time-series measurements of current, voltage, and temperature) as input, and use deep neural networks to automatically learn spatiotemporal features, non-linear coupling relationships, and dynamic evolution patterns embedded in the data, thereby achieving high-precision SOC prediction. Compared to traditional methods, deep learning models can more effectively handle a series of complex dynamic behaviors exhibited by LFP batteries during actual operation, including voltage plateau characteristics, rate-dependent effects, temperature sensitivity, and dynamic transient responses.

3.2.1. Artificial Neural Networks and Deep Neural Networks

Artificial Neural Networks (ANNs) are computational models inspired by biological neural systems, consisting of interconnected neurons that process inputs via activation functions and weighted connections[10]. A typical form is the feed-forward network, which includes an input layer, an output layer, and one or several hidden layers[11]. Shallow ANNs-those with 1 to 3 hidden layers-have been widely used in early state of charge (SOC) estimation studies due to their ability to approximate nonlinear mappings between multi-variable inputs such as current and voltage, and the target output SOC. However, such models exhibit limited capacity in capturing temporal dependencies, are prone to overfitting, and often perform poorly under dynamic conditions or within voltage plateau regions of $LiFePO_4$ batteries.

Deep Neural Networks (DNNs), as a fundamental and widely applied model in deep learning, can be viewed as an extension of shallow ANNs with significantly increased depth. By incorporating more hidden layers, DNNs are capable of combining input features (e.g., current, voltage, temperature) in a higher-order manner, thereby strengthening their ability to model complex nonlinear relationships and enhancing representational power. Despite these advantages, DNNs still lack explicit mechanisms for modeling temporal dependencies. As a result, they generally underperform compared to specialized sequence models such as Recurrent Neural Networks (RNNs), Long Short-Term Memory networks (LSTMs), or Transformers, which are inherently designed to leverage temporal dynamics in time-series data-a critical aspect for accurate SOC estimation under real-world operating conditions.

3.2.2. Convolutional Neural Networks

Convolutional Neural Networks(CNNs) were initially designed as deep learning models for image processing tasks. Their architecture is inspired by biological visual systems and efficiently processes grid-structured data such as images and time-series signals through mechanisms like local perception, weight sharing, and hierarchical feature extraction. Due to their outstanding performance in local feature extraction, CNNs have increasingly been applied to battery State of Charge (SOC) estimation tasks in recent years.

A typical CNNs structure consists of multiple functional layers stacked alternately:

- The input layer receives raw sensor data (e.g., voltage, current, temperature). After preprocessing (e.g., noise filtering, data normalization), the time-series data is often reshaped into an image-like 2D format for subsequent processing.
- The convolutional layer employs multiple convolutional kernels that slide over the input data to perform convolution operations, extracting local features and generating feature maps.
- The activation layer (e.g., ReLU, Leaky ReLU) introduces nonlinear transformation capabilities.
- The pooling layer (e.g., max pooling or average pooling) reduces computational complexity through downsampling while enhancing the model's robustness to minor input variations.
- Finally, the fully connected layer flattens the extracted high-level features and maps them to the output space. The output layer completes the SOC prediction using a Softmax function (for classification) or a linear activation function (for regression) [12],[13].

During model training, CNNs optimize network parameters via the backpropagation algorithm to minimize the error between predicted and true SOC values. This approach is particularly suitable for extracting effective features from local charging and discharging patterns, demonstrating strong application potential especially in scenarios with large datasets and high feature dimensions.

3.2.3. Recurrent Neural Networks

Recurrent Neural Networks (RNNs) belong to a category of neural network models that are specially crafted for handling sequential data, including text, speech, and time - series data. The structure of RNNs consists of an input layer, hidden layers, and an output layer. However, in contrast to feed - forward neural networks like CNNs, RNNs integrate recurrent connections within the hidden layers. This feature allows them to capture the relationships between the present inputs and past information. This self-loop structure allows hidden states to retain a certain "memory," making RNNs effective at capturing dynamic dependencies in time-series data.

Specifically, at each time step "t", an RNN combines the current input with the hidden state from the previous time step and computes the current hidden state through a nonlinear activation function (e.g., tanh or ReLU). This hidden state is then used to generate the corresponding output. The process can be mathematically expressed as follows[14]:

$$h_t=\sigma_h(W_{xh}x_t+W_{hh}h_{t-1}+b_h) \tag{2}$$

$$y_t=\sigma_y(W_{hy}h_t+b_y) \tag{3}$$

Here, W_{xh} denotes the weight matrix from the input layer to the hidden layer, W_{hh} represents the weight matrix for the recurrent connections within the hidden layer, and W_{hy} is the weight matrix from the hidden layer to the output layer. The vectors b_h and b_y are biases for the hidden and output layers, respectively, while σ_h and σ_y are activation functions.

Given that battery SOC is highly correlated with historical charging and discharging behaviors, the recurrent structure of RNNs allows them to leverage hidden states to "memorize" historical information. This enables the model to capture dynamic dependencies among parameters such as voltage, current, and temperature as they evolve during charging and discharging processes, thereby achieving more accurate SOC predictions. However, traditional RNNs suffer from vanishing or exploding gradient problems, making it difficult to effectively capture long-range dependencies, such as battery dynamic processes that span minutes or even hours.

3.2.4. Long Short-Term Memory and Gated Recurrent Unit

As enhanced variants of Recurrent Neural Networks, both Long Short-Term Memory(LSTM) and Gated Recurrent Unit(GRU) architectures were developed to address the issues of vanishing or exploding gradients inherent in traditional RNNs, thereby improving the modeling of long-range temporal dependencies. Their core innovation lies in the introduction of gating mechanisms to dynamically regulate the retention and forgetting of information.

LSTM introduces a "cell state" as a carrier of long-term memory and employs three gating units for precise information control: the forget gate employs a Sigmoid function to decide which past data should be removed from the cell state. Meanwhile, the input gate sifts through fresh information from the present input that needs to be kept and then modifies the cell state accordingly; and the output gate determines the information to be passed to the next time step based on the current cell state and hidden state. This mechanism enables LSTM to flexibly manage information flow, thereby effectively

capturing dependencies in long sequences[15]. The core mechanism of the model can be described by the following six vector equations[16]:

$$c_t=f_t\odot c_{t-1}+i_t\odot\widetilde{c_t} \tag{4}$$

$$\widetilde{c_t}=g(W_c x_t+U_c h_{t-1}+b_c) \tag{5}$$

$$h_t=o_t\odot g(c_t) \tag{6}$$

$$i_t=\sigma(W_i x_t+U_i h_{t-1}+b_i) \tag{7}$$

$$f_t=\sigma(W_f x_t+U_f h_{t-1}+b_f) \tag{8}$$

$$o_t=\sigma(W_o x_t+U_o h_{t-1}+b_o) \tag{9}$$

Equation (4) describes the update method of the current memory cell state, where the forget gate signal f_t and the input gate signal i_t jointly act on the screening and integration of information, where $\odot$ denotes the Hadamard product.. The update process consists of two parts: one is the previous moment's memory cell state c_{t-1} retained by the forget gate, and the other is the newly added candidate memory cell state $\widetilde{c_t}$ filtered by the input gate. Equations (5), (7), (8), and (9) share a unified computational form. In these equations, the output gate signal o_t, along with the gate activation function g (typically the Sigmoid function) and the state activation function σ (such as tanh or ReLU), are used. W and U represent weight matrices, and bias vectors b is also involved. The control signals for the input gate, forget gate, and output gate are all generated through linear transformation and bias addition based on the current input x_t and the previous hidden state h_{t-1}. Equation (6) represents the generation process of the current hidden state h_t: the cell state c_t is processed by an activation function g and then filtered by the output gate o_t to finally determine the hidden information passed to the next time step. LSTM can effectively capture dynamic changes during battery charging and discharging processes, making it particularly suitable for conditions with continuous current variations. However, it suffers from slower training speed, sensitivity to hyperparameters, and high computational complexity.

GRU is a simplified architecture derived from LSTM, reducing the number of parameters by merging gating units while maintaining comparable performance in most cases. GRU replaces the three gates in LSTM with two gating units: the update gate combines the functions of the forget gate and input gate in LSTM, collectively controlling the retention of historical information and the incorporation of new information; the reset gate determines whether to ignore historical information, allowing the model to focus more on the current input. The vector equations of GRU can be expressed as follows[16]:

$$h_t=(1-z_t)\odot h_{t-1}+z_t\odot\widetilde{h_t} \tag{10}$$

$$\widetilde{h_t}=g(W_h x_t+U_h(r_t\odot h_{t-1})+b_h) \tag{11}$$

$$z_t=\sigma(W_z x_t+U_z h_{t-1}+b_z) \quad (12)$$

$$r_t=\sigma(W_r x_t+U_r h_{t-1}+b_r) \quad (13)$$

Here, z_t and r_t represent the update gate signal and reset gate signal, respectively. The meanings of the remaining symbols and the computational flow are similar to the corresponding parts in LSTM and will not be elaborated here.

GRU eliminates the cell state used in LSTM and directly achieves information transfer and updates through the hidden state, resulting in a more concise model structure and higher training efficiency. In many application scenarios, GRU can serve as a lightweight alternative to LSTM, particularly suitable for embedded BMS with limited computational resources or scenarios with high real-time requirements.

3.3. Typical Research Case Analysis

In recent years, purely data-driven methods have demonstrated significant potential in SOC estimation for LFP batteries, achieving breakthroughs in addressing challenges such as voltage plateaus, short-term estimation, and noise interference. Tian et al. proposed a DNN architecture integrating 1D convolution, max pooling, GRU, and fully connected layers. Using only 10 minutes of charging current and voltage sequences, they reduced SOC estimation errors to below 2.03% across the entire SOC range and successfully mitigated the impact of voltage plateaus. The model also exhibited transferability across aging states and battery types, though its validation was limited to the CCCV charging protocol and did not include multi-temperature scenarios[17]. Building on this, Hu et al. systematically compared the performance of DNN under five charging protocols (CCCV, CPCV, MCCCV, PC, and AC) and at different temperatures. Their results showed that, at 25℃, using only 90 seconds of charging data could control SOC errors within 2%, highlighting the stability and practicality of this method under real-world conditions[18].

Liu et al. innovatively introduced force signals as a fourth-dimensional input feature, leveraging the significant mechanical response of LFP batteries in the mid-SOC range to construct a multidimensional LSTM model. Using only 5 seconds of data, they reduced the RMSE to below 0.5%. The model demonstrated excellent generalization capabilities under various dynamic conditions and temperatures, with an online estimation time of less than 1 second. However, the coupling mechanism between force signals and temperature requires further exploration[19]. Hamid et al. employed GRU to process time-series data. Through systematic manual hyperparameter tuning, they maintained errors below 3% even under harsh conditions with systematic current offsets, underscoring the advantages of recurrent neural networks in noise and offset resistance[20]. Park et al. proposed an innovative data representation method that converts 1D voltage and current time-series data into 2D images through grayscale encoding (GS) and utilizes CNN such as ResNet for image regression. This approach achieved high-precision SOC and capacity estimation while reducing model size and computational overhead by over 90% through model pruning and quantization techniques, greatly facilitating the application of the algorithm in resource-constrained embedded BMS[21].

Overall, by employing diverse deep learning architectures (e.g., DNN, LSTM, GRU, CNN) and innovative data utilization strategies (such as short-term charging windows, multimodal sensing signals, and time-series-to-image conversion), purely data-driven methods have made significant progress in the accuracy, robustness, and deployment suitability of SOC estimation for LFP batteries. However, these methods still commonly face challenges such as limited interpretability, high dependency on additional sensing information, and insufficient generalization capability under complex aging states and real-world driving conditions.

4. PHYSICAL-DATA-DRIVEN HYBRID MODELS

Physical-data-driven hybrid models represent a methodology that integrates physics-based modeling with data-driven techniques. This approach retains a simplified representation of the battery's internal mechanisms while leveraging measured data to estimate parameters that are difficult to characterize solely through physical laws. The core idea can be described as "physical structure + data-based adaptation." In the context of SOC estimation for batteries, these models commonly employ equivalent circuit models as their foundational framework to capture voltage dynamics, and integrate state estimation algorithms-such as Kalman filters and observers-to enable real-time inference of internal states including SOC. In recent years, many studies have further enhanced this paradigm by embedding data-driven components like neural networks into the physical model structure. By combining the interpretability of physics-based models with the adaptive capability of machine learning, these approaches achieve significantly improved accuracy in SOC estimation.

Thanks to their computational efficiency, suitability for real-time application, and strong engineering practicality, physical-data-driven hybrid models have emerged as one of the mainstream solutions for SOC estimation in real-world deployments, particularly for LFP batteries.

4.1. Equivalent Circuit Models

In battery modeling, Equivalent Circuit Models(ECMs) exemplify a common hybrid methodology that integrates physics with data. These models utilize networks built from fundamental electrical elements-including resistors, capacitors, and voltage sources-to emulate the dynamic voltage behavior of a battery when subjected to external current stimuli. This type of model does not aim to precisely describe the complex internal electrochemical processes of batteries but instead focuses on an equivalent representation of external characteristics. It utilizes physically interpretable circuit structures to characterize dynamic phenomena such as ohmic polarization and concentration polarization, while commonly relying on measured data to estimate model parameters[22].

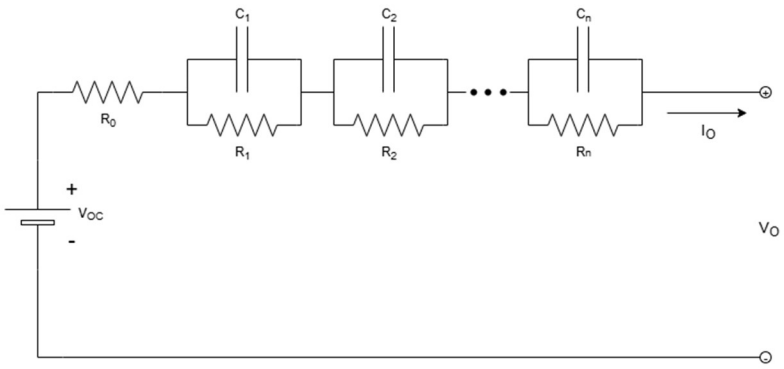

Fig. 2. nRC equivalent circuit model

In SOC estimation studies for LFP batteries, ECMs have become one of the mainstream modeling methods in engineering applications due to their simple structure, ease of parameter identification, low computational burden, and compatibility with various state estimation algorithms. Particularly for LFP batteries, which exhibit distinct voltage plateaus, relatively flat rate responses, and sensitivity to polarization dynamics, well-designed ECMs can effectively capture their dynamic behavior, providing a foundation for high-precision real-time SOC estimation. These models typically include

parallel RC networks composed of resistors and capacitors, with common structures such as the Rint model (0RC), Thevenin model (1RC), and Dual Polarization (DP) model (2RC). Fig. 2 shows the general structure of the nRC model. Additionally, derived structures like the PNGV model, GNL model, and fractional-order models are used to meet the modeling requirements of different application scenarios[23].

4.1.1. Rint Model

The Rint model, representing the simplest form of battery equivalent circuit models, is illustrated in Fig. 3[23]. It consists solely of an open-circuit voltage source (VOC) and an ohmic internal resistance (R0), both of which vary with temperature and state of charge (SOC).

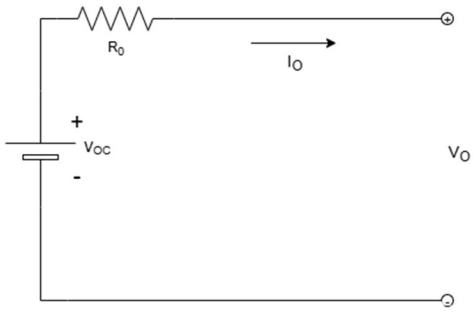

Fig. 3. Rint model

This model captures basic voltage behavior under steady-state conditions and offers high computational efficiency with minimal parameters, making it suitable for applications where dynamic response is not critical. However, by entirely neglecting internal polarization effects and transient dynamics, the Rint model fails to represent key characteristics of LFP batteries-particularly the pronounced voltage hysteresis and recovery behavior during charge and discharge, especially throughout the flat voltage plateau region.

As a result, its accuracy in predicting terminal voltage under real dynamic operating conditions is limited, and it falls short of supporting high-precision SOC estimation. Although valued for its simplicity and ease of implementation, the Rint model is generally confined to roles such as steady-state analysis, baseline comparison, or educational reference, and is not recommended for dynamic SOC estimation of LFP batteries under complex operating conditions.

4.1.2. Thevenin Model

The Thevenin model is currently one of the most widely used, structurally simplest, and most engineering-friendly equivalent circuit models. Its basic structure is illustrated in the fig. 4[23].

In this model, R0 represents the internal ohmic resistance of the battery, covering electrolyte resistance, separator resistance, and contact resistance between current collectors and electrodes. This resistance responds rapidly, generating a voltage drop instantly upon current application. Its value is weakly related to SOC but is susceptible to temperature and aging effects. The parallel RC network composed of R1 (polarization resistance) and C1 (polarization capacitance) describes the polarization phenomena caused by electrochemical reaction kinetics and ion diffusion limitations during charging and discharging, including activation polarization and concentration polarization. The time constant of this network, $\tau = R1 \times C1$, determines the dynamic response speed of the polarization voltage.

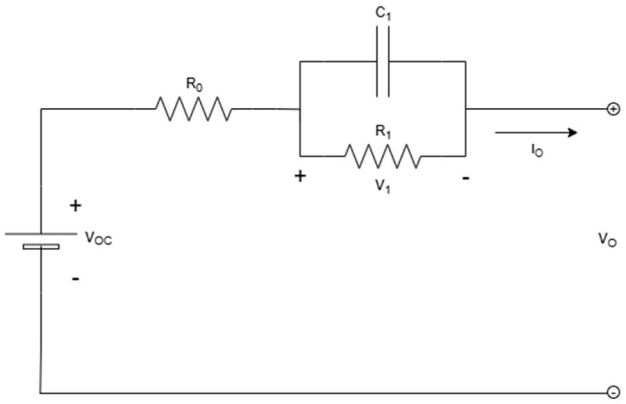

Fig. 4. Thevenin model

The open-circuit voltage source VOC exhibits a nonlinear mapping relationship with SOC, serving as a critical bridge connecting the internal state of the battery with its external terminal voltage. The OCV-SOC curve is typically obtained through offline experimental calibration. For LFP batteries, the mid-range SOC interval features a significant voltage plateau where the OCV changes very gradually. Therefore, higher-precision calibration methods or model-based compensation are often required.

The Thevenin model effectively characterizes the ohmic voltage drop and polarization dynamics of LFP batteries under conventional rates, particularly in describing the slow response characteristics within the plateau region. However, due to the relatively weak polarization effects of LFP materials (compared to high-energy-density materials like NCM), the RC time constant is small. Thus, under high-rate or low-temperature conditions, a single RC network may not fully capture the dynamic behavior of the system. In such cases, the model can be extended to a multi-RC network structure to improve accuracy.

4.1.3. Dual Polarization Model

The DP model, often referred to as the 2RC model, extends the Thevenin equivalent circuit by incorporating an additional RC parallel network, as depicted in Fig. 5[23].

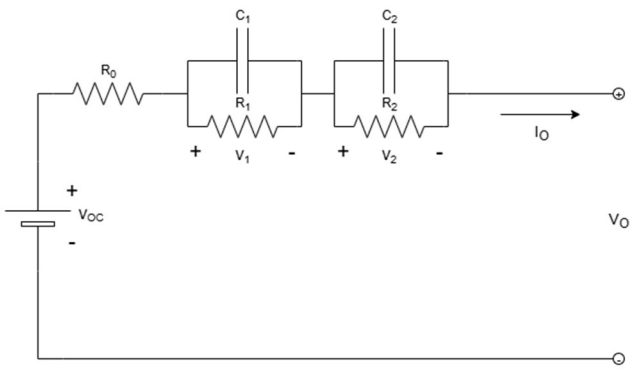

Fig. 5. Dual Polarization model

In this configuration, the first RC network typically represents fast polarization processes-such as electrochemical polarization-while the second accounts for slower dynamics, like concentration polarization.With this structure, the 2RC model offers a more accurate portrayal of the dynamic voltage response during battery operation. It is particularly effective at capturing slow polarization recovery and voltage hysteresis near the flat plateau region of LFP batteries.

Due to the inherently moderate polarization characteristics of LFP materials and their relatively short RC time constants, the 2RC model generally provides high modeling accuracy and reliable SOC estimation under normal operating conditions, including moderate rates and ambient temperatures. It thus represents a balanced compromise between computational efficiency and performance among medium-complexity models.However, under extreme conditions such as high-rate charging/discharging, low temperatures, or high-current pulses, the polarization behavior of LFP cells can deviate from ideal dynamics and evolve more rapidly. In these scenarios, a two-RC network may no longer suffice to capture the full transient response, leading to reduced model accuracy.To better handle such cases, the model can be further expanded to a 3RC or higher-order structure, improving its ability to represent complex polarization dynamics and thereby enhancing the robustness and adaptability of SOC estimation.

4.2. State Estimation Algorithms

Equivalent electrical circuit models are capable of precisely depicting the external dynamic characteristics of batteries. Nevertheless, as the state of charge (SOC) is an internal state parameter that cannot be directly gauged, it is crucial to utilize state estimation algorithms based on the theory of dynamic systems. By integrating equivalent circuit models with measurable voltage and current signals, these algorithms enable real-time inference of the battery's internal state through recursive computation.

In SOC estimation for LFP batteries, a series of Kalman filtering techniques and their improved variants-based on nonlinear system theory-have been widely applied within the framework of equivalent circuit models. These algorithms constitute a core technical pathway in physical-data-driven hybrid SOC estimation methods. Through the establishment of state-space equations for the battery and the incorporation of real-time current and voltage measurements, they achieve high-precision and adaptive SOC estimation. Given the characteristics of LFP batteries-such as a flat voltage plateau, relatively mild polarization response, and dynamics highly sensitive to temperature and aging effects-these state estimation algorithms are required to possess enhanced nonlinear processing capability, robustness against disturbances, and adaptive parameter tuning.

4.2.1. Extended Kalman Filter

The Extended Kalman Filter(EKF) is an extension of the classical Kalman Filter for nonlinear systems. This method achieves local linearization by performing a first-order Taylor expansion of the nonlinear system equations and conducts state prediction and update within the linear Kalman Filter framework. The state-space model of a general nonlinear system can be expressed as follows[6]:

$$x_{k+1}=f(x_k,u_k)+d_k \tag{14}$$

$$y_k=g(x_k,u_k)+s_k \tag{15}$$

In SOC estimation, the state vector x_k includes system state variables such as SOC at time k; the input u_k and output y_k represent observable signals such as current I_k and terminal voltage V_k, respectively; $f(x_k, u_k)$ and $g(x_k, u_k)$ are the nonlinear state transition function and observation function, respectively;

while d_k and s_k denote process noise and measurement noise, typically modeled as zero-mean Gaussian white noise. The EKF algorithm consists of two core steps: the prediction step, which uses the state equation f to provide a prior estimate of the state and covariance at the next time step, and the update step, which leverages the observation equation g and the actual measured voltage to correct the state estimate via the Kalman gain.

The advantage of EKF lies in its relatively simple implementation, moderate computational requirements, ease of deployment on embedded platforms, and mature technical foundations with well-established parameter calibration methods. However, its limitations include the reliance on Jacobian matrix calculations for linearization, which may introduce significant errors, as well as sensitivity to initial errors and limited robustness. For LFP batteries, EKF is suitable for SOC estimation under conventional operating conditions, particularly performing well in dynamic regions outside the voltage plateau. In flat OCV regions, however, high-precision OCV-SOC curves or joint estimation strategies are often required to ensure estimation accuracy.

4.2.2. Unscented Kalman Filter

The Unscented Kalman Filter(UKF) abandons the traditional Jacobian-based linearization method and instead employs the Unscented Transform (UT). To carry out state estimation within nonlinear systems, it chooses a group of deterministic sample points (Sigma points). These points precisely represent the mean and covariance of the state distribution. After propagation through the nonlinear system, these Sigma points can still effectively reflect the statistical characteristics of the posterior distribution. Compared to EKF, UKF avoids the computation of Jacobian matrices, more accurately preserves the nonlinear characteristics of the system, and thus generally achieves higher estimation accuracy, making it particularly suitable for strongly nonlinear systems. The implementation of the standard UKF primarily involves the following four steps:

- Sigma Point Generation: Generate a set of sample points based on the current state and its covariance;
- Sigma Point Propagation: Propagate the sample points through the nonlinear state equation and observation equation, respectively;
- Statistical Reconstruction: Recalculate the posterior mean and covariance of the state based on the propagated point set;
- State Update: Use the actual observed values to correct the state via the Kalman gain[6].

UKF demonstrates significant advantages in handling SOC estimation for LFP batteries within the plateau region, as it can more accurately describe the nonlinear mapping relationship between OCV and SOC. However, the estimation accuracy and computational complexity of UKF are both influenced by the number of Sigma points. Its implementation is also more complex than that of EKF, and its scaling parameters and weighting coefficients must be carefully selected to maintain numerical stability.

4.2.3. Particle Filter

The Particle Filter (PF) relies on the Monte Carlo simulation approach. It makes use of a collection of randomly selected particles, each assigned a weight, to estimate the posterior probability distribution of the system's state. It is particularly suitable for systems with non-Gaussian, strongly nonlinear, or complex distributions. Each particle represents a possible state value (e.g., SOC), and its estimation accuracy is significantly influenced by the number of particles. The basic workflow of the algorithm consists of the following three steps:

- Prediction: Based on the system state equation, the particle states at time k are predicted using the particle swarm at time k-1 and the current input (e.g., current). Process noise is typically added during this step to account for model uncertainties and input measurement errors.

- Update: The theoretical observed values of each particle are calculated according to the observation equation and compared with the actual measured values. The weights of the particles are then adjusted accordingly, ensuring the total weight remains normalized to 1. By assigning higher weights to particles with better matching degrees, the credibility of the estimation results is effectively enhanced.
- Resampling: As iterations proceed, particle weights may degenerate, meaning a few particles dominate with high weights while most approach zero, leading to a loss of sample diversity. To address this, resampling is performed based on the weights, retaining high-weight particles and eliminating low-weight ones. After resampling, the weights of all particles are reset to 1/n (where n is the total number of particles)[24].

PF does not require linearization of the system, exhibits strong resistance to non-Gaussian noise, and can be compatible with battery models of varying complexity, making it widely applicable. When a sufficient number of particles is used, its estimation accuracy is high; however, a large number of particles significantly increases computational burden, posing higher requirements for the computing power of onboard BMS. Additionally, even though resampling mitigates degeneracy, there remains a risk of reduced particle diversity, which may further impact estimation accuracy.

4.3. Typical Research Case Analysis

In response to the significant hysteresis observed during the charging and discharging processes of LFP batteries, several research teams have proposed improvements in modeling and estimation methods from different perspectives. Ko et al. replaced the traditional parallelogram hysteresis model with a piecewise linearized hysteresis contour model, combined with a simplified 2RC equivalent circuit and EKF filtering, achieving an RMSE of 0.69% in the SOC plateau region. However, the effects of temperature and dynamic operating conditions were not considered[25]. Antony et al. introduced a Hysteresis Correction Factor (HCF) based on a second-order RC model, dynamically compensating for hysteresis voltage and significantly improving estimation accuracy under various conditions. Nonetheless, the HCF factor still relies on experimental calibration and has limited adaptive capability[26].

At the algorithm level, Hossain et al. systematically compared nonlinear Kalman filtering algorithms such as EKF, AEKF, UKF, and AUKF, highlighting that the RLS-AUKF combination performed optimally across a wide temperature range (-5°C to 45°C), with an MAE of only 0.9%. However, their study did not cover aging state evaluation or embedded real-time validation[6]. To further address nonlinear issues in low SOC regions, Huang et al. proposed an adaptive piecewise equivalent circuit model, achieving partitioned identification of electrochemical and thermal parameters using dual EKF. Their approach achieved an explanation degree exceeding 95% across a wide temperature range and enabled joint estimation of SOC and SOH, though the partitioning strategy still requires manual presetting[27].

Addressing the unique SOC plateau characteristics of LFP batteries, teams led by Xiong and Peng independently proposed methods based on OCV slope partitioning. Xiong et al. combined online ARSR identification with an EKF segment start-stop strategy, controlling the maximum absolute error within 2%[28]. Peng's team further introduced a temperature compensation factor (Tc) and employed PID combined with an improved AEKF for partitioned collaboration, achieving a 54% improvement in convergence speed while maintaining errors below 3%. However, both studies insufficiently investigated aging and extreme temperature scenarios[29]. Yi et al. focused on voltage measurement deviations (ΔV) in the plateau region, proposing a partitioned compensation algorithm based on high-pass filtering and DEKF, which significantly improved SOC estimation in flat regions but did not account for current sensor biases[30].

Furthermore, some scholars have expanded modeling approaches from the perspective of physical dynamic responses. Zhu et al. introduced variable time constant RC branches or even RLC circuits

into traditional RC hysteresis models to simulate relaxation and overshoot effects. Combined with TCKF, they achieved high-precision estimation of complex dynamic behaviors, though comparisons with other classical filtering algorithms were lacking[31]. Umar's team pioneered the integration of fractional-order models with dynamic hysteresis effects, employing fractional-order DEKF to simultaneously estimate multiple state parameters. Their approach achieved an MAE below 1.5% across multiple temperatures. Although computationally complex, it provides valuable insights for high-precision BMS design[32].

Although physical-data-driven hybrid methods based on equivalent circuit models demonstrate strong engineering practicality and computational efficiency in battery SOC estimation, they inherently rely on simplified assumptions about the internal dynamic behavior of batteries. These include limited RC network structures, linear or fixed-parameter kinetic descriptions, and static OCV-SOC relationships. Such simplifications often struggle to accurately capture actual dynamic characteristics under complex conditions such as high-rate charging/discharging, low-temperature environments, battery aging, and the flat voltage plateau region unique to LFP batteries, leading to reduced SOC estimation accuracy.

To address these limitations, researchers have increasingly turned to enhanced hybrid modeling strategies that further integrate data-driven techniques. This approach retains the mechanistic structure and interpretability of equivalent circuit models while incorporating more advanced machine learning methods to compensate for model errors, unmodeled dynamics, or complex nonlinear mappings. By doing so, it significantly enhances the accuracy and generalization capability of SOC estimation while maintaining real-time performance and engineering feasibility.

Chen et al. constructed a four-hidden-layer DNN model for SOC estimation of LFP batteries and employed a Kalman filter based on physical equations to smooth and denoise the DNN outputs. This DNN-KF hybrid model achieved an MAE below 2% and an RMSE below 2.4% across multiple temperatures, reducing errors by 10%–25% compared to a pure DNN approach. It demonstrated good convergence and computational efficiency meeting real-time requirements, though its adaptability in low-temperature and aging scenarios requires further validation[33]. Wei et al. proposed a closed-loop estimation framework that coulomb counting as the state equation and a NARX dynamic neural network as the observation equation, with Sage-Husa adaptive Kalman filtering introduced for online correction. Under various LFP battery types, dynamic conditions, and temperatures, this model achieved SOC estimation errors below 2%, an RMSE below 1%, and an MAE lower than 0.74%, performing particularly well in the nonlinear plateau region[34]. Peng et al. utilized an LSTM network optimized with a random weights algorithm (RW) and applied adaptive weighted EKF (AWEKF) to filter and optimize the SOC outputs. The RW-LSTM-AWEKF model maintained high accuracy across a wide temperature range from -10°C to 50°C, highlighting its practical potential for onboard BMS applications[35].

While the aforementioned methods partially circumvent equivalent circuit model errors, they exhibit relatively weak interpretability. In contrast, Hou et al. retained the Rint equivalent circuit model combined with EKF for coarse SOC estimation and employed XGBoost for residual error correction. This strategy prioritizes the mechanistic model supplemented by data-driven techniques, enhancing both accuracy and interpretability[36]. Chen et al. proposed a "voltage shielding" strategy: first, a reverse first-order RC equivalent circuit model (RFORC-ECM) was used to fit interpretable dynamic voltage components and output a noisy OCV_n; then, an LSTM-RNN was adopted to establish a nonlinear mapping between OCV_n, current, temperature, and SOC to address residual dynamics. This hybrid architecture significantly improved the fitting stability of the LSTM through physical preprocessing, though its capabilities in handling aging and online updating require further enhancement[37].

In summary, research on physical-data-driven hybrid modeling for LFP batteries predominantly revolves around the integration of hysteresis characteristic compensation and state estimation

algorithms. By developing dynamic hysteresis voltage models, adopting piecewise fitting strategies, and incorporating advanced nonlinear observers, significant improvements have been achieved in SOC estimation performance within the plateau region. However, several key challenges remain: on one hand, model parameters (e.g., hysteresis coefficients, RC parameters) largely rely on offline calibration, with limited online adaptive adjustment capabilities, restricting their applicability to aged batteries and across full temperature ranges; on the other hand, the characterization of relaxation dynamics and aging evolution mechanisms specific to LFP materials is still insufficient. Future research should prioritize the development of collaborative online identification methods for parameters and states, enhance model adaptability under varying aging states and temperature scenarios, and explore deeper integration with data-driven strategies. This will further improve accuracy and robustness under complex practical conditions while maintaining model interpretability.

5. RESULTS AND DISCUSSION

This review systematically analyzes and compares the performance and applicability of different SOC estimation models for LFP batteries. The analysis reveals distinct performance characteristics for each model category.

Purely data-driven models, including DNNs, LSTMs, CNNs, and Transformers, demonstrate superior capability in capturing the complex, nonlinear behaviors of LFP chemistry, such as the flat voltage plateau and significant hysteresis. These models achieve high estimation accuracy under conditions well-represented in their training data. However, the results indicate significant drawbacks, including a lack of model interpretability, a heavy dependency on the quantity and quality of training data, and substantial computational requirements. These limitations currently restrict their practical deployment in real-time, resource-constrained BMS hardware.

In contrast, physical-data-driven hybrid models, primarily Enhanced ECMs integrated with state estimators like Kalman filters, show a more balanced performance profile. They provide satisfactory computational efficiency and maintain a degree of physical interpretability, making them the current industry standard for BMS implementation. The discussion confirms that recent enhancements, such as incorporating hysteresis compensation and adaptive algorithms, have notably improved their accuracy. Nevertheless, the performance of these models is still constrained by their reliance on offline parameter identification and demonstrates degradation under extreme operational scenarios, particularly at very low/high temperatures and throughout severe battery aging.

6. CONCLUSION

This review concludes that accurate SOC estimation for LFP batteries remains challenging due to their unique electrochemical properties. The study's primary findings confirm that no single modeling approach currently offers a perfect solution; purely data-driven models provide high accuracy at the cost of interpretability and computational load, while hybrid models offer robustness and real-time capability but face limitations in generalization.

Based on this analysis, future research should prioritize the development of more adaptive hybrid modeling strategies that deeply integrate mechanistic understanding with data-driven learning. Key directions include advancing online parameter identification to accommodate battery aging, enhancing model robustness across diverse and extreme operating conditions, and optimizing advanced algorithms for efficient deployment on embedded BMS platforms. Such integrated efforts are essential for achieving the reliable, high-precision SOC estimation required for the next generation of electric vehicles and energy storage systems.

REFERENCES

[1] Nyamathulla, S., & Dhanamjayulu, C. (2024). A review of battery energy storage systems and advanced battery management system for different applications: Challenges and recommendations. Journal of Energy Storage, 86, 111179.

[2] Rostami, H., Valio, J., Tynjälä, P., Lassi, U., & Suominen, P. (2024). Life cycle of LiFePO4 batteries: production, recycling, and market trends. ChemPhysChem, 25(24), e202400459.

[3] Selvaraj, V., & Vairavasundaram, I. (2023). A comprehensive review of state of charge estimation in lithium-ion batteries used in electric vehicles. Journal of Energy Storage, 72, 108777.

[4] Dreyer, W., Jamnik, J., Guhlke, C., Huth, R., Moškon, J., & Gaberšček, M. (2010). The thermodynamic origin of hysteresis in insertion batteries. Nature materials, 9(5), 448-453.

[5] Padhi, A. K., Nanjundaswamy, K. S., & Goodenough, J. B. (1997). Phospho-olivines as positive-electrode materials for rechargeable lithium batteries. Journal of the electrochemical SOCiety, 144(4), 1188.

[6] Hossain, M., Haque, M. E., & Arif, M. T. (2022). Kalman filtering techniques for the online model parameters and state of charge estimation of the Li-ion batteries: A comparative analysis. Journal of Energy Storage, 51, 104174.

[7] Lai, X., Sun, L., Chen, Q., Wang, M., Chen, J., Ke, Y., & Zheng, Y. (2024). A novel modeling methodology for hysteresis characteristic and state-of-charge estimation of LiFePO4 batteries. Journal of Energy Storage, 101, 113807.

[8] Barai, A., Widanage, W. D., McGordon, A., & Jennings, P. (2016, June). The influence of temperature and charge-discharge rate on open circuit voltage hysteresis of an LFP Li-ion battery. In 2016 IEEE Transportation Electrification Conference and Expo (ITEC) (pp. 1-4). IEEE.

[9] Wang, X., Zhang, Y., Deng, Y., Yuan, Y., Zhang, F., Lv, S., ... & Ni, H. (2023). Effects of different charging currents and temperatures on the voltage plateau behavior of li-ion batteries. Batteries, 9(1), 42.

[10] Wu, Y. C., & Feng, J. W. (2018). Development and application of artificial neural network. Wireless Personal Communications, 102(2), 1645-1656.

[11] Dongare, A. D., Kharde, R. R., & Kachare, A. D. (2012). Introduction to artificial neural network. International Journal of Engineering and Innovative Technology (IJEIT), 2(1), 189-194.

[12] Ajit, A., Acharya, K., & Samanta, A. (2020, February). A review of convolutional neural networks. In 2020 international conference on emerging trends in information technology and engineering (ic-ETITE) (pp. 1-5). IEEE.

[13] Li, Z., Liu, F., Yang, W., Peng, S., & Zhou, J. (2021). A survey of convolutional neural networks: analysis, applications, and prospects. IEEE transactions on neural networks and learning systems, 33(12), 6999-7019.

[14] Mienye, I. D., Swart, T. G., & Obaido, G. (2024). Recurrent neural networks: A comprehensive review of architectures, variants, and applications. Information, 15(9), 517.

[15] Al-Selwi, S. M., Hassan, M. F., Abdulkadir, S. J., Muneer, A., Sumiea, E. H., Alqushaibi, A., & Ragab, M. G. (2024). RNN-LSTM: From applications to modeling techniques and beyond-Systematic review. Journal of King Saud University-Computer and Information Sciences, 36(5), 102068.

[16] Dey, R., & Salem, F. M. (2017, August). Gate-variants of gated recurrent unit (GRU) neural networks. In 2017 IEEE 60th international midwest symposium on circuits and systems (MWSCAS) (pp. 1597-1600). IEEE.

[17] Tian, J., Xiong, R., Shen, W., & Lu, J. (2021). State-of-charge estimation of LiFePO4 batteries in electric vehicles: A deep-learning enabled approach. Applied Energy, 291, 116812.

[18] Hu, C., Ma, L., Guo, S., Guo, G., & Han, Z. (2022). Deep learning enabled state-of-charge estimation of LiFePO4 batteries: A systematic validation on state-of-the-art charging protocols. Energy, 246, 123404.

[19] Liu, M., Xu, J., Jiang, Y., & Mei, X. (2023). Multi-dimensional features based data-driven state of charge estimation method for LiFePO4 batteries. Energy, 274, 127407.

[20] Hamid, M. (2023). Deep learning with Hyperparameter optimisation for SOC estimation of LFP cells. Authorea Preprints.

[21] Park, H., Kim, Y. S., & Shin, Y. J. (2024, October). Real-time state estimation of lithium-ion battery using image-based regression with CNN. In 2024 10th International Conference on Condition Monitoring and Diagnosis (CMD) (pp. 390-393). IEEE.

[22] Lai, X., Zheng, Y., & Sun, T. (2018). A comparative study of different equivalent circuit models for estimating state-of-charge of lithium-ion batteries. Electrochimica Acta, 259, 566-577.

[23] Mishra, S., Swain, S. C., & Samantaray, R. K. (2021, October). A Review on Battery Management system and its Application in Electric vehicle. In 2021 International conference on advances in computing and communications (ICACC) (pp. 1-6). IEEE.

[24] Schwunk, S., Armbruster, N., Straub, S., Kehl, J., & Vetter, M. (2013). Particle filter for state of charge and state of health estimation for lithium–iron phosphate batteries. Journal of Power Sources, 239, 705-710.

[25] Ko, Y., & Choi, W. (2021). A new soc estimation for lfp batteries: Application in a 10 ah cell (hw 38120 l/s) as a hysteresis case study. Electronics, 10(6), 705.

[26] Antony, A. J., & Kamakshy, S. (2024, June). Extended Kalman Filter Based Estimation of the State of Charge of Lithium Iron Phosphate Battery Using an Equivalent Circuit Model. In 2024 6th International Conference on Energy, Power and Environment (ICEPE) (pp. 1-6). IEEE.

[27] Huang, Z., Best, M., Knowles, J., & Fly, A. (2022). Adaptive piecewise equivalent circuit model with SOC/SOH estimation based on extended Kalman filter. IEEE Transactions on Energy Conversion, 38(2), 959-970.

[28] Xiong, R., Duan, Y., Zhang, K., Lin, D., Tian, J., & Chen, C. (2023). State-of-charge estimation for onboard LiFePO4 batteries with adaptive state update in specific open-circuit-voltage ranges. Applied Energy, 349, 121581.

[29] Peng, S., Zhang, D., Dai, G., Wang, L., Jiang, Y., & Zhou, F. (2025). State of charge estimation for LiFePO4 batteries joint by PID observer and improved EKF in various OCV ranges. Applied Energy, 377, 124435.

[30] Yi, B., Zhang, J., & Song, Z. (2024, July). Bias-compensated state estimation algorithm for lithium iron phosphate batteries with flat OCV-SOC curves. In 2024 American Control Conference (ACC) (pp. 1423-1428). IEEE.

[31] Zhu, G., Wu, O., Wang, Q., Kang, J., & Wang, J. V. (2023). The modeling and SOC estimation of a LiFePO4 battery considering the relaxation and overshoot of polarization voltage. Batteries, 9(7), 369.

[32] Umar, A., Mukhopadhyay, S., & Patra, A. (2024). Improved State of Charge estimation of a Li-ion cell using a Fractional Order Model with hysteresis. Journal of Energy Storage, 103, 114114.

[33] Chen, G., Jiang, S., Xie, M., & Yang, F. (2022, October). A hybrid DNN-KF model for real-time SOC estimation of lithium-ion batteries under different ambient temperatures. In 2022 Global Reliability and Prognostics and Health Management (PHM-Yantai) (pp. 1-5). IEEE.

[34] Wei, M., Ye, M., Zhang, C., Lian, G., Xia, B., & Wang, Q. (2024). Robust state of charge estimation of LiFePO4 batteries based on Sage_Husa adaptive Kalman filter and dynamic neural network. Electrochimica Acta, 477, 143778.

[35] Peng, J., Takyi-Aninakwa, P., Wang, S., Masahudu, F., Yang, X., & Guerrero, J. M. (2024). A hybrid-aided approach with adaptive state update for estimating the state-of-charge of LiFePO4 batteries considering temperature uncertainties. Journal of Energy Storage, 76, 109758.

[36] Hou, J., Xu, J., Lin, C., Jiang, D., & Mei, X. (2024). State of charge estimation for lithium-ion batteries based on battery model and data-driven fusion method. Energy, 290, 130056.

[37] Chen, J., Li, K., Liu, W., Yin, C., Zhu, Q., & Tang, H. (2025). A novel state of charge estimation method for LiFePO4 battery based on combined modeling of physical model and machine learning model. Journal of Energy Storage, 115, 115888.